

RESEARCH

Open Access



# Computer aided design of novel antibiotic drug candidate against multidrug resistant strains of *Salmonella typhi* from pyridine-substituted coumarins

Philip John Ameji<sup>1\*</sup> , Adamu Uzairu<sup>2</sup>, Gideon Adamu Shallangwa<sup>2</sup> and Sani Uba<sup>2</sup>

## Abstract

**Background** The rising cases of resistance to existing antibiotics by *Salmonella typhi*, has made the development of novel drug candidates a necessity. In this study, a data set of antibacterial pyridine substituted coumarins were subjected to Virtual Screening against SipA effector protein of the bacterium. The compounds were geometry-optimized using Semi-empirical (pm3) method in Spartan 14 software, docked against the active sites of SipA using AutoDock Vina software. The molecule with the best docked score was selected as template and subjected to structural modifications leading to the design of a novel coumarin based drug candidate codenamed Y-1.

**Results** The docking of Y-1 against SipA revealed that it binds to the target with  $\Delta G$  value of  $-9.1$  kcal/mol. This value is better than  $-6.8$  kcal/mol obtained for ciprofloxacin used herein for quality assurance. Additionally, quantum mechanical calculations on Y-1 using DFT (B3LYP/6-31G\* basis set) shows a wide energy gap of 3.44 eV and  $\omega$  value of 1.47 eV, indicating its sound kinetic and thermodynamic stabilities. Y-1 was also found to possess good oral bio-availability and positive pharmacokinetic profiles.

**Conclusion** This is the first time coumarin derivatives are screened against an effector protein of *Salmonella typhi*. It is envisaged that the findings of this research will provide an excellent blueprint toward the development of novel antibiotics against *Salmonella typhi*.

**Keywords** Typhoid fever, SipA, DFT, In-silico, *Salmonella typhi*

## 1 Background

At its earlier stage, the application of Computational Chemistry techniques to solve real life challenges faced some drawbacks owing principally to poor sophistication in computer software and hardware. However, with advancement in computing technology, these challenges

are gradually been surmounted. A significant milestone in this research area is the use of Computer Aided Drug Design strategies to develop novel drugs such as Captopril, Dorzolamide, Saquinavir, Zanamivir, Oseltamivir, Aliskiren, Boceprevir, Nilotrexed, TMI-005, LY-517717, Rupintrivir and NVP-AUY922, many of which have either been approved or in clinical trials [1]. Just quiet recently, Martin Karplus of Harvard University, US, Michael Levitt of Stanford University, US, and Arieh Warshel of the University of Southern California, US, were awarded Nobel Prize in Chemistry for applying Computational Chemistry techniques to model complex chemical systems. By applying quantum and classical calculations to different

\*Correspondence:

Philip John Ameji  
ameji.john@fulokoja.edu.ng

<sup>1</sup> Department of Chemistry, Federal University Lokoja, P.M.B. 1154, Lokoja, Kogi State, Nigeria

<sup>2</sup> Department of Chemistry, Ahmadu Bello University, P.M.B. 1044, Zaria, Kaduna State, Nigeria



© The Author(s) 2024. **Open Access** This article is licensed under a Creative Commons Attribution 4.0 International License, which permits use, sharing, adaptation, distribution and reproduction in any medium or format, as long as you give appropriate credit to the original author(s) and the source, provide a link to the Creative Commons licence, and indicate if changes were made. The images or other third party material in this article are included in the article's Creative Commons licence, unless indicated otherwise in a credit line to the material. If material is not included in the article's Creative Commons licence and your intended use is not permitted by statutory regulation or exceeds the permitted use, you will need to obtain permission directly from the copyright holder. To view a copy of this licence, visit <http://creativecommons.org/licenses/by/4.0/>.

parts of a single molecule, the trio developed Molecular Dynamics (MD) technique that mimic the real life movement of complex entities like proteins and electrostatic calculations which could compute the attractive or repulsive force between charged atoms and molecules [2]

A major cause of illnesses and increased death rate in human population is infections by pathogenic bacteria. The rapid evolution of various adaptive strategies to antibiotics by these organisms has led to development of multidrug resistance strains of the pathogens, an ugly circumstance that is on the verge of overwhelming the pharmaceutical industry due to its inability to keep up with the ever increasing demand for effective novel antibacterial drugs [3]. The situation is so critical that it has been projected that by the year 2050, the annual death rate attributable to antibiotic resistance could be as high as 10 million [4].

Of particular concern in this study is the rising cases of antibiotic resistance in *Salmonella typhi*, an anaerobic Gram-negative bacterium responsible for Typhoid fever infection. This disease is prevalent in economically disadvantaged countries with poor health care systems and has an estimated global annual morbidity and mortality rates of 12–27 million and 116, 800 respectively. It is transmitted through the fecal–oral route, infecting the intestine and the blood of the host [5–8]. The major clinical manifestations of Typhoid fever include fever, abdominal discomfort, and several gastrointestinal complications, such as nausea, vomiting, constipation, and diarrhea. In severe cases, it leads to gastro intestinal perforation, bleeding, and neurological complications [9–11].

Chloramphenicol, ampicillin and cotrimoxazole were the first antibiotics of resort for the treatment of typhoid fever infection [12]. The resistance to these first line antibiotics by *Salmonella typhi* led to the deployment of quinolone and  $\beta$ -lactam antibiotics. Regrettably, the emergence of quinolone and  $\beta$ -lactam resistant strains of this bacterium is currently a major public health concern globally [13, 14]. Resistance to the former is through point mutations in quinolone resistance-determining regions (QRDR) orchestrated by the acquisition of the genes; topoisomerase IV (*parC* and *parE*) and DNA gyrase (*gyrA* and *gyrB*) while resistance to the latter is via the acquisition of the *bla*TEM gene that encode the  $\beta$ -lactamase enzyme that hydrolyzes the peptide bond of the  $\beta$ -lactam ring, preventing the antibiotics from wielding their effects [15–19]. In the light of the foregoing, it has become expedient to search, discover, and develop novel antibacterial agents with better potencies and different mechanisms of action from the existing ones.

The conventional drug discovery and development approach is a herculean task because of the enormous time and resources expended in the process. However,

the application of in silico techniques as a complementary strategies help to circumvent these bottlenecks. One of these techniques is application of structure based drug design (SBDD). In SBDD, the 3D structure of the target protein is known, and following molecular docking simulation studies, the binding affinities of tested compounds to the target are calculated, paving way for the design of novel therapeutic molecule with better binding to the target protein [20, 21]. Furthermore, ADME/T defines the Absorption, Distribution, Metabolism, Excretion and Toxicity of a therapeutic compound. The success of a drug in clinical trials is greatly dependent on these properties. Computer aided ADME/T profiling of drug candidates is therefore an essential component of modern drug design as early prediction of these properties in drug candidates help minimize attrition rate in drug development [22, 23].

*Salmonella typhi* will ordinarily not be able to survive in the intestine when ingested by its host (human) because of the harsh conditions of the extracellular milieu orchestrated by factors such as low pH, shear stress due to mucosal secretions or blood and host defense mechanisms. Thus, Central to its pathogenesis is the ability to invade the intestines of its host and gains entry into the tissues where it replicates rapidly and manifest varying degree of virulence [24, 25]. The invasion of this organism into the host cell is influence by type-3-secretion effector protein known as SipA. This it does by binding directly to actin, a major protein constituent of cytoskeleton, cooperating with the pathogen to promote the formation of actin filaments at the site of bacterial adhesion, and prevent filament disassembly by host factors [26]. Furthermore, tight junctions are specialized cell junctions that bounds epithelial cells lining the small intestine and prevent even small molecules from passing into the lumen. The integrity of these junctions is maintained by two major transmembrane proteins, claudins and occludins. *Salmonella typhi* with the aid of its SipA effector protein compromises the structures of these junctions during infection by decreasing the amount of phosphorylated occludin, leading to diarrhea and other pathogenic effects [27, 28]. Likewise, after internalization, *Salmonella typhi* creates its intracellular niche in an exclusive membrane-bound compartment known as the *Salmonella* containing vacuole (SCV) where it replicates comfortably [29]. The intermediate stage of the biogenesis of SCV is governed by SipA effector protein.

Coumarins constitute a crucial member of benzopyrone class of compounds with diverse structural features and profound biological and pharmacological properties. Their bioactivities include antibacterial, antifungal and insecticidal properties. Also, coumarins could be used as anticoagulants, antithrombotic, HIV inhibitors and

human progesterone receptor agonists. They are essential components of established drugs. For instance, Novobiocin and Chlorobiocin are approved coumarin based antimicrobial drugs [30–33].

In view of the fundamental roles SipA effector protein plays in *Salmonella typhi*'s virulence and pathogenicity, its inhibition by bioactive compounds is undoubtedly a rational drug discovery strategy. Thus, this study is aimed at the design of novel antagonists of SipA protein of *Salmonella typhi* using computer-aided drug design techniques. The application of these techniques has led to the design of a novel coumarin based drug candidate (Y-1) with strong antagonistic potential against SipA protein of *Salmonella typhi*. The novel ligand, Y-1 was also found to exhibit sound ADMET profile. This is the first time coumarin analogs are screened against an effector protein, SipA, of *Salmonella typhi*.

## 2 Methods

### 2.1 Data collection and geometry optimization

In this work, a total of 25 leads were obtained from recent literature [34]. The inhibitory activities of the leads were measured using the same experimental procedures and a wide range of inhibitory activities were covered. The 2D structure of the molecules were drawn with ChemDraw V12.0 and imported into Spartan'14 software ([www.wavefun.com](http://www.wavefun.com)) interface where they were converted to 3D. The ligands were geometry-optimized using the Semi-empirical (pm3) method and subsequently saved as PDB and sdf file formats for further analysis. The structures of the leads and their anti-*Salmonella typhi* inhibitory activities are presented in Table 1.

### 2.2 Virtual screening

Virtual screening involves the use of computational methods to analyze databases of bioactive compounds with the sole aim of identifying potential hit candidates. The computational method deployed here for screening the data set of the investigated bioactive molecules is Molecular Docking simulation, a technique that allows accurate prediction of the strength of association or binding affinity between the leads (ligands) and the target protein (SipA). With the aid of AutoDock Vina software, the optimized ligands were prepared and saved as pdbqt files. The three-dimensional crystal of SipA protein with protein data bank code of 1q5z was obtained from [www.rcsb.org/pdb](http://www.rcsb.org/pdb). The heteroatoms and water molecules attached to the protein target were removed using the Discovery Studio v2016. Polar hydrogens and Kollman charges were added to the prepared protein, non-polar hydrogen were removed, and missing atoms were checked and repaired using the AutoDock Vina tool v1.5.7. Furthermore, the dimensions of the grid box were generated to cover all

the residues of the enzyme and docking was performed using EasyDock vina v2.2. Lastly, the modes of interaction of the ligands with the residual amino acids of the macromolecule were investigated using the Discovery Studio Visualizer v16.1.0.15350 [35].

### 2.3 Design of new ligands

Design of novel ligands is necessarily in order to obtain analog with enhanced potency. Here, the molecule with the best dock score (lowest  $\Delta G$  value) was selected as template. The molecular features of the template molecule vital for its binding specificity against the SipA enzyme known as its pharmacophores were noted via the analysis of the diagram of interaction of the molecule with the target enzyme. The pharmacophores were modified to give a newly designed analog named Y-1. The designed compound and a standard antibiotic (Ciprofloxacin) used for quality assurance were further subjected to molecular docking simulation against the active sites of SipA protease target using the same procedures for the lead molecules described in Sect. 2.2 [35].

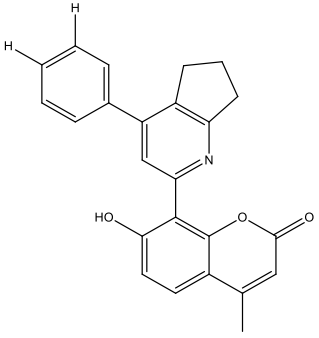
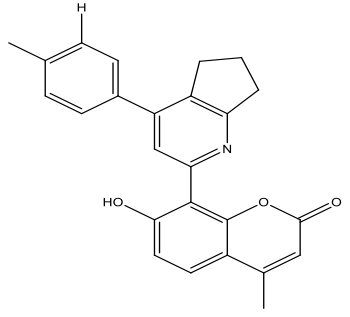
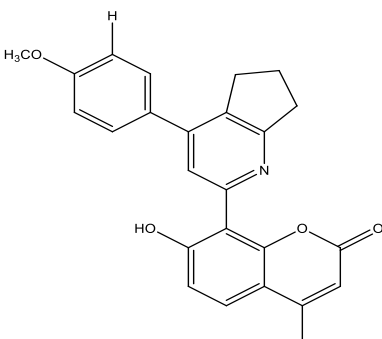
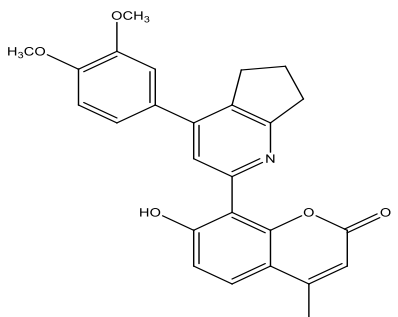
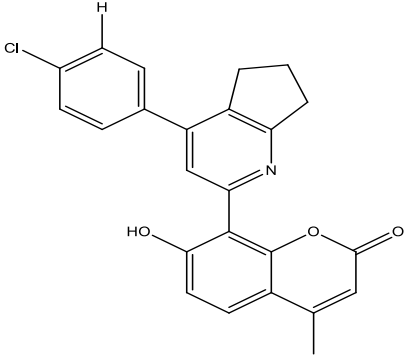
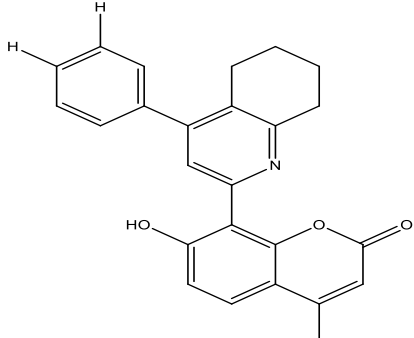
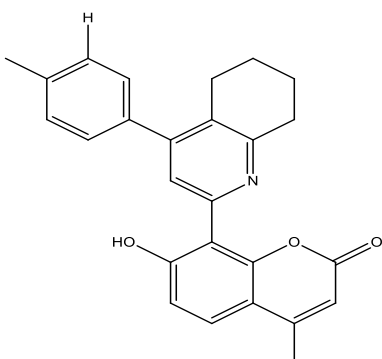
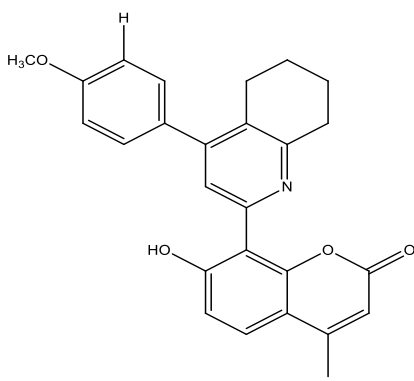
#### 2.3.1 Drug-likeness assessment of the designed compound

Drug-likeness assesses the suitability of a therapeutic molecules for oral administration. This vital insilico assessment was done on ligand Y-1 using the famous Lipinski's rule of five and the Veber's rules. According to Lipinski's rule, a drug would most likely be orally bioavailable if it obeys at least three of the following conditions; molecular weight (MW)  $\leq 500$  g/mol, number of hydrogen bond donors (HBD)  $\leq 5$ , octanol/ water partition coefficient  $\log P \leq 5$  and number of hydrogen bond acceptors (HBA)  $\leq 10$  [30]. The Veber's rule on the other hand states that for a drug to be orally bioavailable, the number of rotatable bonds (NRB) must be  $< 10$  and topological polar surface area (TPSA) must be  $< 140 \text{ \AA}^2$  [36, 37]. The physicochemical descriptors of drug likeness of Y-1 ligand was computed with the aid of SwissADME tool at [www.swissadme.ch/](http://www.swissadme.ch/) DataWarrior V5.5.0 chemo-informatics tool.

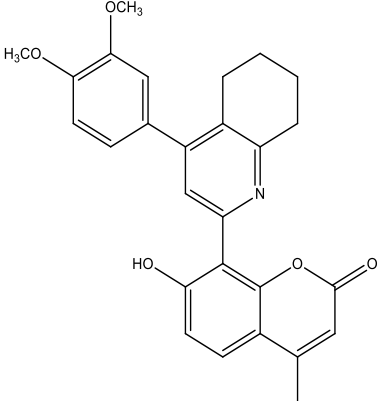
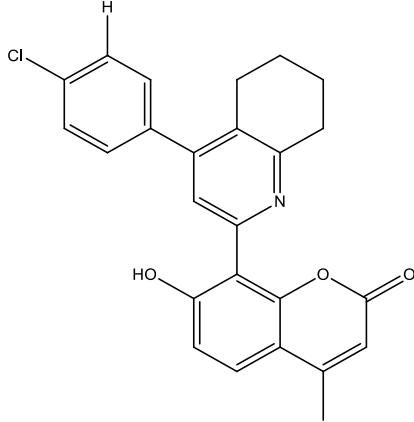
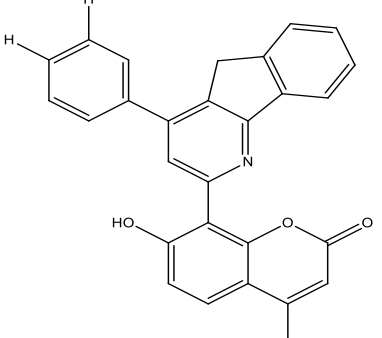
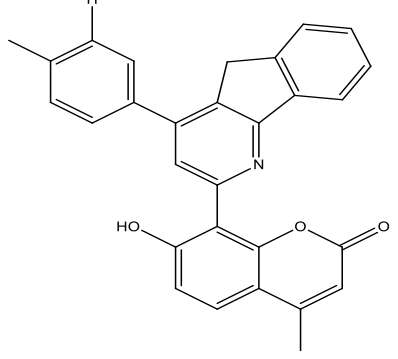
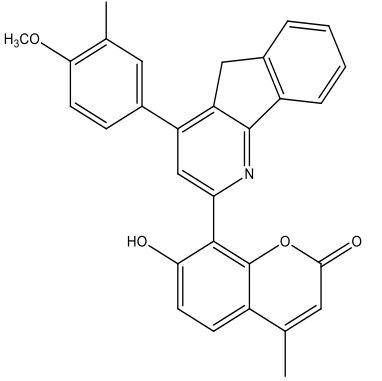
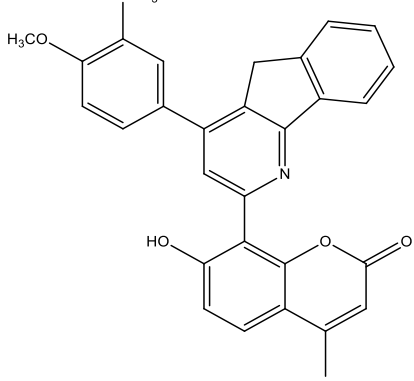
#### 2.3.2 ADME/T estimate

ADME/T is a pharmaceutical acronym that deals with chemical Absorption (A), Distribution (D), Metabolism (M), Excretion (E) and Toxicity (T) of a therapeutic compound. The success of a drug in clinical trials is greatly dependent on these properties. Insilico ADME/T profiling of drug candidates is therefore an essential component of modern drug design [38, 39]. ADME/T profiles of Y-1 was computed using SwissADME ([www.swissadme.ch/](http://www.swissadme.ch/) accessed on 21 September, 2022) and DataWarrior V5.5.0 chemoinformatics program.

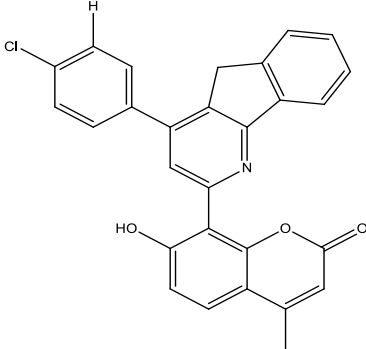
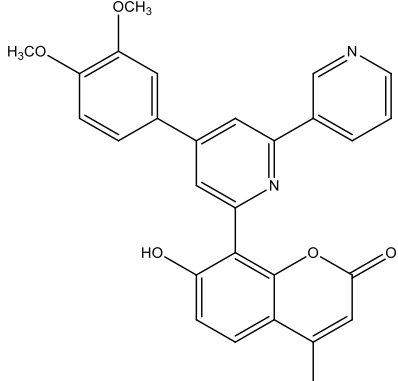
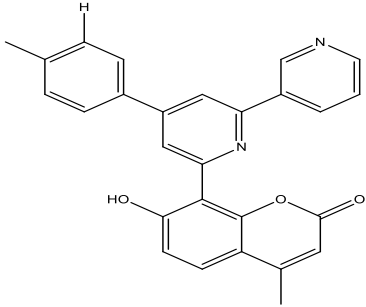
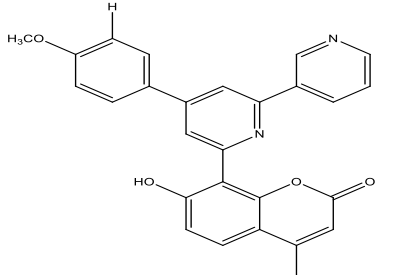
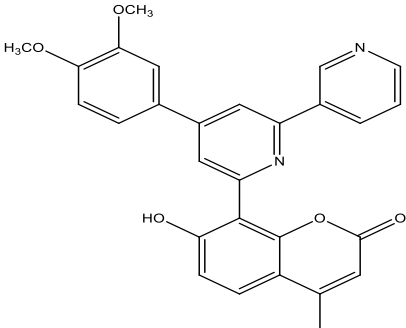
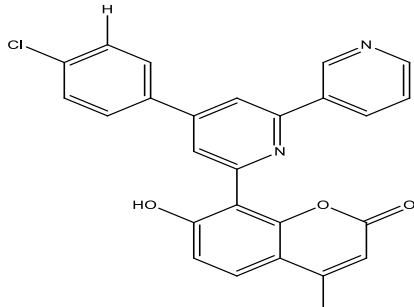
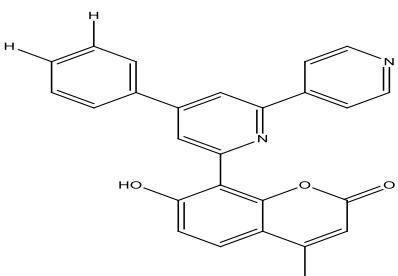
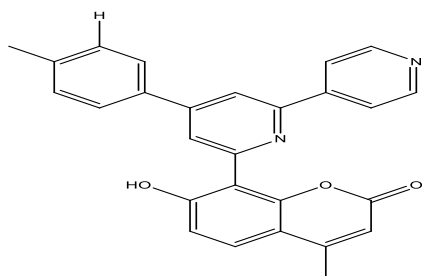
**Table 1** 2D structures and Invitro MIC values of the investigated compounds

S/n	Structure	MIC ( $\mu\text{g/mL}$ )	S/n	Structure	MIC ( $\mu\text{g/mL}$ )
1		200	2		500
3		250	4		200
5		500	6		200
7		63	8		500

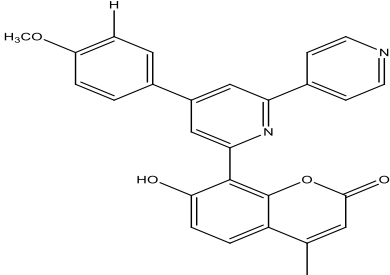
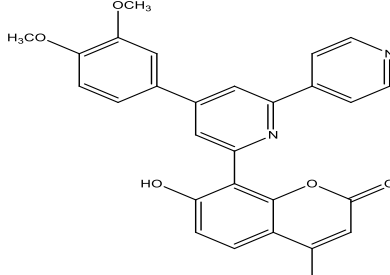
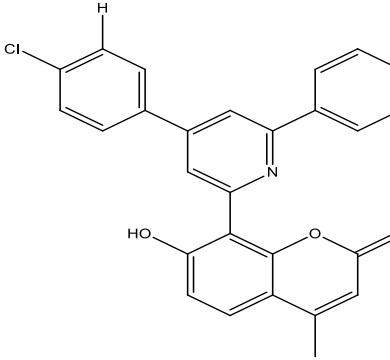
**Table 1** (continued)

S/n	Structure	MIC ( $\mu\text{g/mL}$ )	S/n	Structure	MIC ( $\mu\text{g/mL}$ )
9		100	10		500
11		200	12		250
13		100	14		250

**Table 1** (continued)

S/n	Structure	MIC ( $\mu\text{g/mL}$ )	S/n	Structure	MIC ( $\mu\text{g/mL}$ )
15		500	16		200
17		250	18		50
19		100	20		200
21		200	22		250

**Table 1** (continued)

S/n	Structure	MIC ( $\mu\text{g/mL}$ )	S/n	Structure	MIC ( $\mu\text{g/mL}$ )
23		500	24		100
25		100			

### 2.3.3 Quantum mechanical calculation on the designed compound

The Spartan'14 software ([www.wavefun.com](http://www.wavefun.com)) was used to perform quantum calculations on ligand Y-1. Geometry optimization and frequency calculations were carried out using DFT alongside the B3LYP standard principle in conjunction with the split-valence 6-31G\*\* basis function. The choice of this method is anchored on its computational efficiency and high accuracy in obtaining geometries, zero-point energy (ZPE) and frequencies [40–42].

The chemical and physical stability of drugs are crucial to their overall quality and safety. Due to the important roles the frontier molecular orbitals plays in molecular stability, their assessment forms an integral component of pharmaceutical research [43]. The frontier molecular orbitals is made up of the highest occupied molecular orbital (HOMO) and Lowest unoccupied molecular orbital (LUMO). The LUMO serves as electron acceptor with an associated energy expressed as electron affinity (EA), while the HOMO plays the role of electron donors and its energy is linked to ionization potential (IP). The charge transfer interaction within a molecule is explained by the HOMO–LUMO energy gap defined in Eq. 1. This energy gap helps to ascertain the electrical transport system within the molecule. A high frontier orbital energy gap in a molecule connotes low chemical reactivity and

high kinetic stability due to the fact that the addition of electrons from the low lying HOMO to high lying LUMO is not energetically feasible [41, 44].

$$\Delta E(\text{Energy gap}) = E_{\text{LUMO}} - E_{\text{HOMO}} \quad (1)$$

where  $E_{\text{LUMO}}$  and  $E_{\text{HOMO}}$  denote energy of LUMO and energy of HOMO, respectively.

Aside the application of HOMO–LUMO energy gap as a measure of stability, another parameter based on thermodynamic properties of molecules is the global electrophilicity index ( $\omega$ ).  $\omega$  refers to the reduction in energy of a system when electrons flow from the HOMO to the LUMO of a molecule. Equation 2 presents the mathematical equation for computing the value of  $\omega$  in a molecule.

$$\omega = \frac{\mu^2}{2\eta}, \quad (2)$$

where  $\eta$  is the global chemical hardness and  $\mu$  the electronic chemical potential which describes the charge transfer within a system in the ground state. Equations 3 and 4, defines  $\eta$  and  $\mu$ , respectively.

$$\eta = \frac{E_{\text{LUMO}} - E_{\text{HOMO}}}{2} \quad (3)$$

$$\mu = \frac{E_{\text{LUMO}} + E_{\text{HOMO}}}{2} \quad (4)$$

Low value of  $\omega$  connotes decreased molecular reactivity and sound thermodynamic stability of a molecule [41].

### 3 Results

#### 3.1 Molecular docking assessment of lead molecules

Design of strong antagonists of SipA enzyme is a rational modern drug discovery strategy owing to the prominent roles this effector protein plays in the pathogenesis and virulence of *Salmonella typhi* in the host cells. The result of molecular docking simulation performed on the synthesized bioactive pyridine-substituted coumarins against the SipA protease of the bacterium is presented in Table 2. The magnitude of the interaction between the compounds and the target

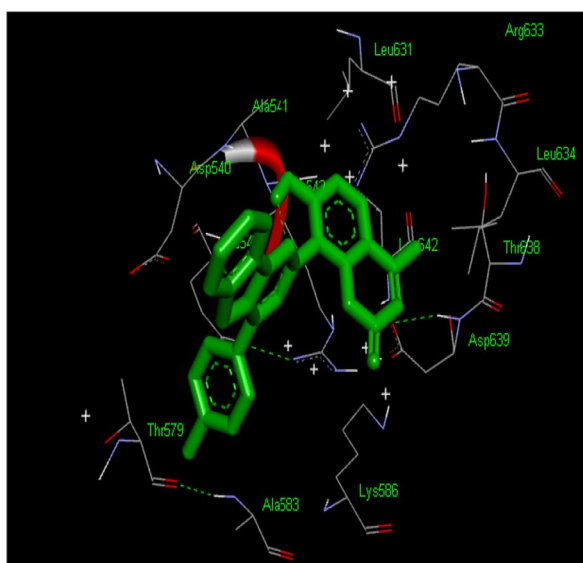
**Table 2** Binding affinity values of the pyridine-substituted coumarins with SipA target protein

S.no	$\Delta G$ (kcal/mol)	S.no	$\Delta G$ (kcal/mol)	S.no	$\Delta G$ (kcal/mol)
1	-8.3	10	-8.3	19	-8.1
2	-8.1	11	-8.5	20	-8.1
3	-8.1	12	-8.6	21	-8.1
4	-8.0	13	-8.4	22	-8.3
5	-8.1	14	-8.3	23	-8.1
6	-8.4	15	-8.5	24	-8.1
7	-8.4	16	-8.0	25	-8.1
8	-8.2	17	-8.1		
9	-8.1	18	-8.0		

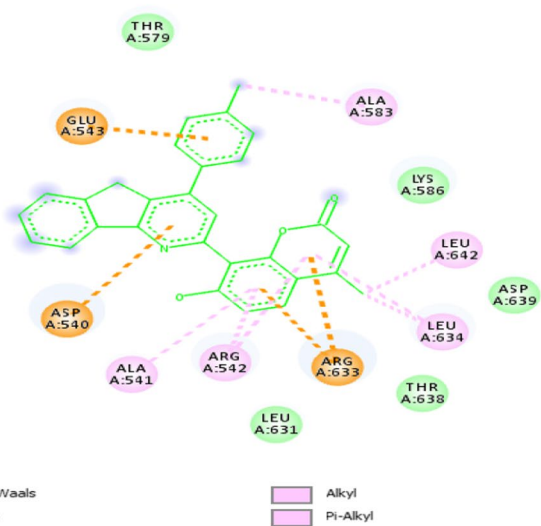
protein was expressed as change in Gibb's free energy of binding ( $\Delta G$ ). The more negative the value of  $\Delta G$  the higher the binding affinity. However, because compounds 12 displayed the best  $\Delta G$  value, it was selected as template for designing more potent derivatives of pyridine-substituted coumarins. The 2D and 3D diagram of interaction of the template molecule is presented in Fig. 1.

#### 3.2 The designed ligand

The aggregation of the steric and electronic features of a molecule that enhances its interaction with macromolecular target constitutes its pharmacophores. Careful evaluation of the diagram of interaction of the template with the target protease in Fig. 1 reveals the pharmacophoric influence of the conjugated cyclic rings on the binding interaction of the ligands. For enhanced binding affinity of newer moieties, the structure of the template was modified via the attachment of cyclopentadiene ring. Also, the presence of hydrogen bond in a protein–ligand complex is necessary owing to the stabilizing effect of the association. Conventional hydrogen bond is absent in the complex of the template with SipA protease (Fig. 1). Hence, hydroxyl functional group was also attached to the parent moiety. These structural adjustments led to the design of a more potent analog codenamed Y-1 whose 2D chemical structure and that of ciprofloxacin (CiproF) are shown in Fig. 2. The 2D and 3D interaction of Y-1 and Ciprofloxacin with the active sites of SipA protease are displayed by Fig. 3, while their binding affinity values and IUPAC names are presented in Table 3.



**Fig. 1** 3D and 2D diagram of the template in complex with SipA protease ( $\Delta G = -8.6$  kcal/mol)





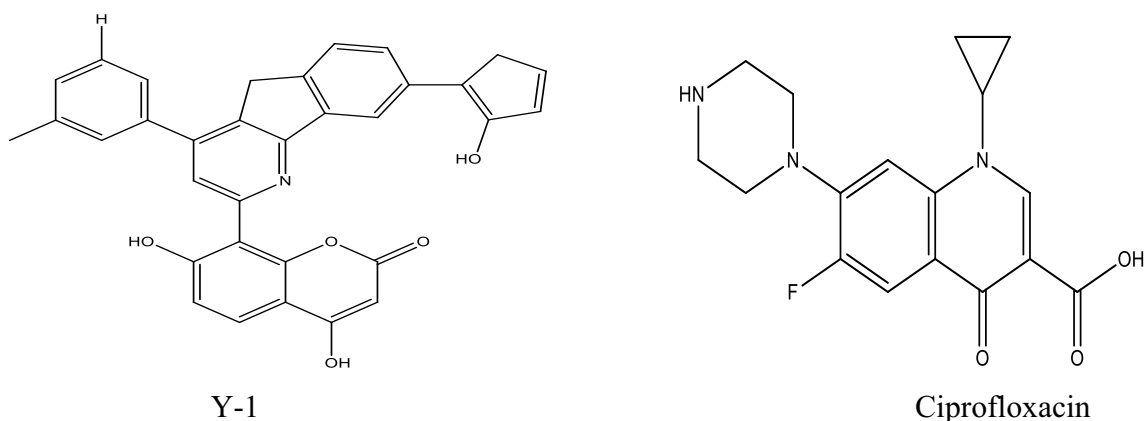
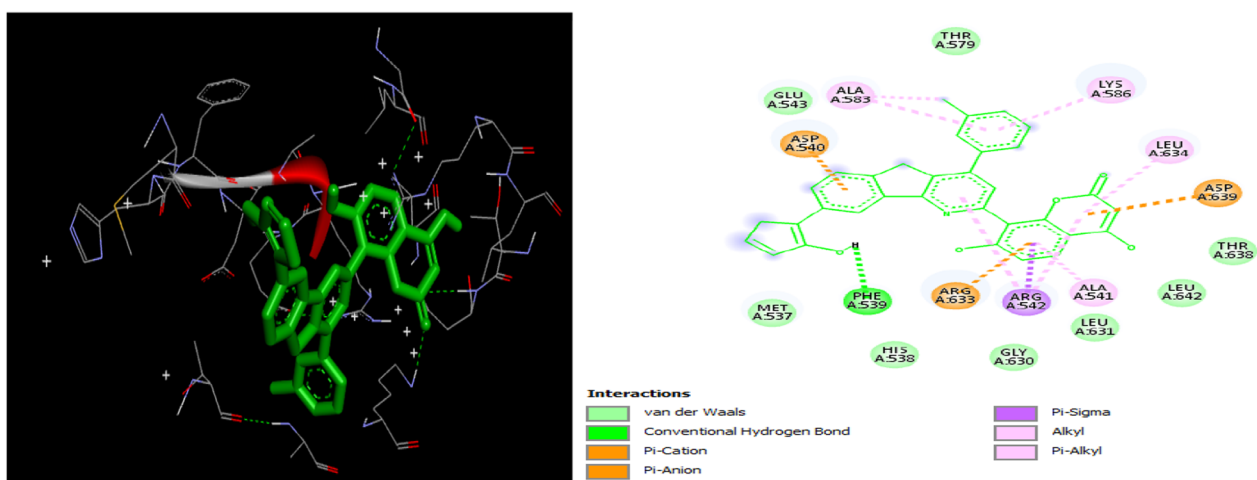
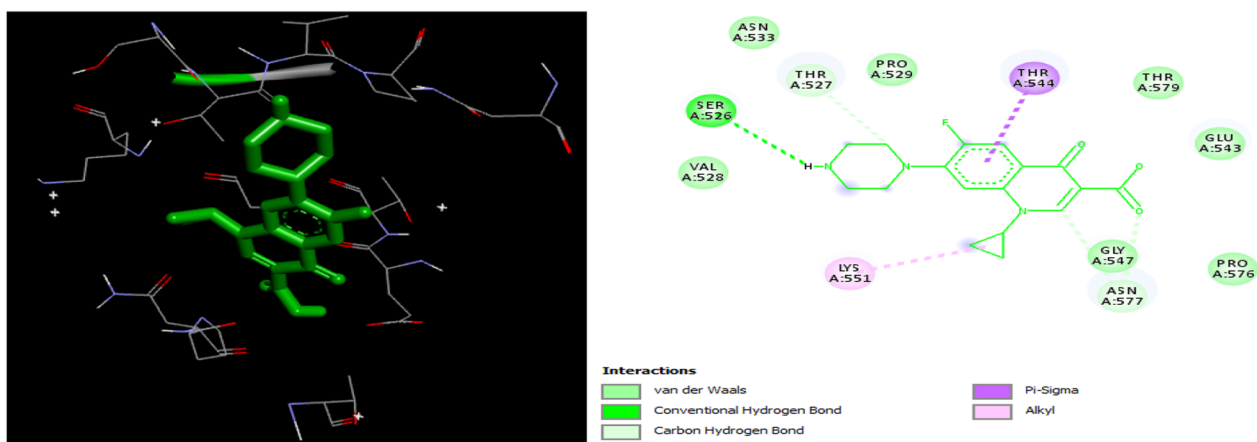


**Fig. 2** 2D chemical structures of the novel ligand and Ciprofloxacin



**A:** Y-1 in complex with active sites of SipA protein target ( $\Delta G = -9.1$  kcal/mol)



**B:** Ciprofloxacin in complex with active sites of SipA protein target ( $\Delta G = -6.8$  kcal/mol)

**Fig. 3** 3D and 2D diagram of the designed compound and ciprofloxacin in complex with the active sites of SipA protease

**Table 3** binding affinity values and IUPAC names of Y-1 and Ciprofloxacin

Compound ID	$\Delta G$ (kcal/mol)	IUPAC name
Y-1	-9.1	4,7-dihydroxy-8-(8-(2-hydroxycyclopenta-1,3-dien-1-yl)-4-(m-tolyl)-5H-indeno[1,2-b]pyridin-2-yl)-2H-chromen-2-one
CiproF	-6.6	1-cyclopropyl-6-fluoro-4-oxo-7-(piperazin-1-yl)-1,4-dihydroquinoline-3-carboxylic acid

### 3.2.1 Oral bioavailability, pharmacokinetic, and toxicity profiles of ligand Y-1 and ciprofloxacin

Drug-likeness and ADMET profiles of bioactive compounds are grossly influenced by certain physicochemical descriptors. These descriptors are computed for Y-1 and the reference antibiotic. The results are presented in Table 4.

### 3.2.2 The computed electronic properties of Y-1

Figure 4 presents the shape and energy plots of the frontier orbitals of the designed ligand while the descriptors of its reactivity are listed in Table 5.

## 4 Discussions

### 4.1 Virtual screening of the bioactive compounds

Actin filaments (polymers of actin) are protein filaments in the cytoplasm of eukaryotic cells that constitute a portion of the cytoskeleton. They engulf particles in addition to providing mechanical support and shape to the cell. SipA protease of *Salmonella typhi* enhances the invasion of the bacterium into the host cell by binding to actin, cooperate with the bacterium to form actin filament at the site of bacterial adhesion and prevent filament disassembly by host factors [30]. This enzyme also causes disruption of tight junctions leading to diarrhea and other pathogenic effects in addition to promoting biogenesis of *Salmonella* containing vacuole [32, 33, 40]. Thus, this enzyme plays important roles in the virulence and pathogenicity of *Salmonella typhi*, making it a target of drug candidates [45]. In the light of this, molecular docking simulation was performed on the studied

compounds to examine the binding affinity values with SipA protease. The result of the investigation presented in Table 2 reveals that compounds 12 with  $\Delta G$  value of -8.6 exhibits the best binding affinity with the active sites of the protease and was selected as template molecule for the design of more potent analog. Investigation of the diagram of interaction (Fig. 2) reveals that the conjugated cyclic rings are the major pharmacophores of the compounds. The lipophilic character of the conjugated ring system could be responsible for enhanced contact with the target protein.

### 4.2 The newly designed ligand

In a bid to design more potent pyridine-substituted coumarins with strong antagonistic potentials against the SipA protease of the bacteria, the template molecule was subjected to pharmacophoric modifications leading to the design of Y-1 (Fig. 2) with binding affinity value of -9.1 kcal/mole (Table 3). These novel ligand displays more potent than the standard ligand, ciprofloxacin having binding affinity value of -6.8 kcal/mol against the target protease. Assessment of the diagram of interaction of the designed ligand and ciprofloxacin with active sites of SipA shown in Fig. 3 revealed that Y-1 binds to the target protein via hydrophobic interaction with ALA583, ALA541, ARG542, LEU634, and LYS586 in alkyl and pi-alkyl types of interaction. Also, cation and pi-cation interactions were observed with ASP540, ARG633, and ASP639. These interactions were stabilized by a conventional hydrogen bond with PHE539 amino acid residue of the protease. Furthermore, the

**Table 4** Drug-likeness and ADMET profiles of the designed ligand

Ligand	Mw	MlogP	LogS	TPSA	NRB	HBA	HBD	Toxicity	Pharmacokinetic
Y-1	513.5	3.52	-6.92	108.9	3	6	3	M: No T: No R: No	CYP450 Substrate: Yes P-gp substrate: No GIA: Yes BBB: No
CiproF	331.3	1.28	-1.32	74.57	3	5	2	M: No T: No R: No	CYP45 Substrate: Yes P-gp substrate: Yes GIA: Yes BBB: No

Mw molecular weight, TPSA topological polar surface area, NRB number of rotatable bond, HBA hydrogen bond acceptor, HBD hydrogen bond donor, M mutagenicity, T tumorigenic effect, R reproductive effect, GIA gastrointestinal absorption, P-gp P-glycoprotein, BBB blood brain barrier

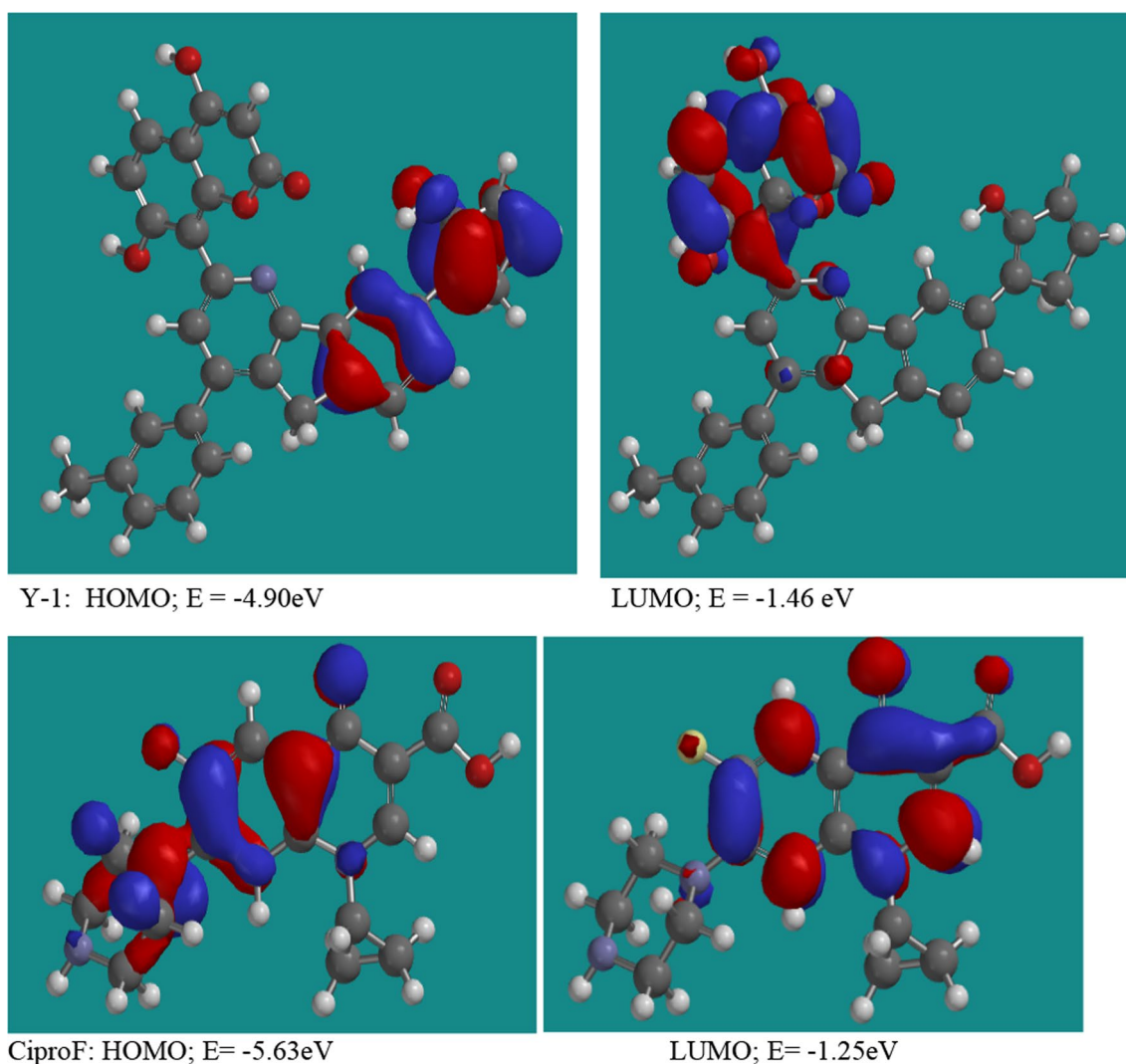


**Fig. 4** The shapes and energy plot of the HOMO and LUMO orbitals of Y-1 and CiproF

**Table 5** Global reactivity descriptors of Y-1

Ligand	HOMO (eV)	LUMO (eV)	$\Delta E$ (eV)	$\mu$ (eV)	$\eta$ (eV)	$\omega$ (eV)
Y-1	-4.9	-1.46	3.44	-3.18	1.72	1.47
CiproF	-5.63	-1.25	4.38	-3.44	2.19	2.70

standard inhibitor, ciprofloxacin displayed the least interaction with the active sites of the target protein. The ligands bind to SipA enzyme through hydrophobic interactions with THR527, THR544, LYS551 and van der Waals interactions with GLY547. These associations were stabilized by conventional hydrogen bond with SER526 amino acid residue of the protease.

In medicinal chemistry, addition of cyclic ring system to a bioactive moiety increases its lipophilic appeal. The increased binding affinity of Y-1 ligand could be as a result of additional lipophilic character and hydrogen bonding tendency of the ligand due to added cyclopentadiene ring bearing hydroxyl group. Also, the novel ligand in addition to possessing higher potency than

the reference Ciprofloxacin antibiotic, exhibits different mechanisms of action against the protein target (SipA) of the bacterium.

#### 4.3 Assessment of drug-likeness of the designed compound

Drug-likeness evaluation is necessarily considering the fact that majority of drugs are taken via oral administration. *In-silico* drug-likeness assessment promotes a cost effective and time-saving drug design strategy that helps to scientifically establish a bioactive compound as a promising drug candidate [46, 47]. The descriptors of drug-likeness of ligand Y-1 presented in Table 4 shows that it obeys the Lipinski's rule of five because it does not violate more than one of the basic parameters stipulated by the rule. Also, the ligand was found to obey the Veber's rule as its TPSA and NRB were found to be less than 140 Å and 10, respectively. Hence, Y-1 could be an orally bioavailable drug candidate. In addition, the oral bioavailability parameters of Y-1 were found to be similar to those of the standard CiproF ligand as both compounds were found to obey the Lipinski's rule of five and the Veber's rule.

#### 4.4 Pharmacokinetic and toxicity evaluation of the designed ligand

Pharmacokinetics basically takes into cognizance the absorption (*A*), distribution (*D*), metabolism (*M*), and excretion (*E*) of drugs in the biological system [48]. Poor pharmacokinetic profiles of drug is responsible for high attrition rate in pharmaceutical companies. Hence, *in-silico* profiling of ADME properties of bioactive compounds prior to *in vitro* studies is a cost effective and time saving strategy in modern drug discovery and development. The *in-silico* pharmacokinetic data (Table 4) of the designed ligand showed that it has good gastrointestinal absorption and could permeate across the intestinal lining of humans.

Also, P-glycoprotein (P-gp) are membrane transporters that protects the body from harmful substances by extruding via efflux action, substrate xenobiotic absorbed in the intestines back to the lumen, removing drugs from the kidneys and liver into the urine and bile respectively, and maintaining integrity of BBB by limiting cellular uptake of its substrates from blood circulation into the brain [49]. The efflux action of P-gp could also influence the ADMET properties of drug leading to its altered efficacy and consequently posing various adverse effect due to possible drug-drug interactions [49]. The pharmacokinetic profile of Y-1 presented in Table 4 reveals that the novel ligand is non-substrates of P-glycoproteins. Thus, its serum concentration will be unaffected by the efflux action of the transporter.

Furthermore, Cytochrome P450 (CYP450) refers to group of enzymes that regulates drug biotransformation, drug interaction, and their elimination from the biological system. Inhibition of these enzymes by any therapeutic molecule could result to delayed removal, severe toxicity, and failure of the drug in the human body [50, 51]. Interestingly, Y-1 was found to be substrate of these enzymes. Hence it could be inferred that the novel drug candidate would be presumably well distributed, metabolized, and excreted in the biological system.

Likewise, *in-silico* toxicity assay on ligand Y-1 to ascertain its mutagenicity, tumorigenic tendency, and effect on reproductive system (Table 4) revealed that Y-1 has an excellent toxicity profile as it is neither mutagenic nor tumorigenic, and displayed no effect on the reproductive health.

As an *in-silico* quality control measure, the pharmacokinetic and toxicity data of Y-1 were compared with those of the standard ligand, CiproF (Table 4). The designed ligand was found to display similar ADMET profiles with the reference ligand. *In-silico* toxicity profiling of both ligands revealed that they are none mutagenic, none tumorigenic, and has no effect on the reproductive system. Also, they are both substrates of CYP450 enzymes and do not permeate the BBB. In addition, Y-1 is found to be a non-substrate of P-gp unlike the standard ligand, CiproF.

#### 4.5 Electronic properties of Y-1

Currently, DFT represents a widely accepted and well known post-Hartree–Fock approach used for *ab initio* calculation of energies and electronic structures of molecules [52]. Analysis of the LUMO and HOMO diagram of Y-1 shown in Fig. 4 reveals that the portion of the ligand where hydroxylated cyclopentadiene ring bonds with the benzene ring represent the HOMO region. The electron donating effect of the hydroxyl group and the pi-electron ring systems may have caused the high electron density in this region of the molecule.

Similarly, the region of the molecule containing Pyran-2-one fused with benzene ring represents the LUMO section of the designed ligand. The inductively electron withdrawing effect of benzyl ether and the electron withdrawing effect of the ketone group by inductive and resonance effects may be the likely cause of reduce electron density of this region of the ligand. The computed energy gap of 3.44 eV for Y-1 (Table 5) reveals a wide  $\Delta E$  value, indicating the low chemical reactivity and high kinetic stability of the therapeutic compound. Additionally, global electrophilicity index ( $\omega$ ) which is a function of  $\eta$  and  $\mu$ , measures the ability of a molecule to take up electrons and it is a measure of thermodynamic stability of molecules. The low value of computed  $\omega$  (1.47 eV) for

Y-1 is an indication of good thermodynamic stability of the designed anti-*Salmonella typhi* drug candidate. The  $\eta$  measures the resistance of a molecule to deformation in its electron density while  $\mu$  accounts for the tendency of electrons to leave a molecule. The most reactive molecule is characterized by high value of  $\mu$  and low value of  $\eta$  [53]. As a quality control measure, the electronic properties of the Y-1 was compared with that of the standard ligand (CiproF). The closeness of the values of  $\Delta E$ ,  $\mu$ ,  $\eta$ , and  $\mu$  for both ligands (Table 5) confirms possible similarity of kinetic and thermodynamic stability of the molecules.

## 5 Future research plan and study limitation

This study is limited to in silico investigations only. However, in furtherance of this research, in vitro and in vivo studies would be performed on the designed ligand, Y-1, in order to validate the findings of the in silico studies.

## 6 Conclusion

The rising incidences of resistance to existing antibiotics by *Salmonella typhi* has necessitated constant search for novel drug candidates in the drug development pipeline. In this study, a series of bioactive pyridine-substituted coumarins were virtually screened against a crucial protein of the bacterium (SipA) using Molecular Docking techniques. The ligands were found to possess binding affinity ( $\Delta G$ ) values ranging from  $-8.0$  to  $-8.6$  kcal/mol. Ligand 12 with  $\Delta G$  of  $-8.6$  kcal/mol displayed the best inhibitory role against the target macromolecule and was selected as template molecule. Structural modification of the template led to the design of more potent derivative (ligand Y-1) with  $\Delta G$  value of  $-9.1$  kcal/mol against the target protein. When compared with Ciprofloxacin ( $\Delta G = -6.6$  kcal/mol), the novel ligand was found to be more potent. In-silico drug-likeness and ADMET assays on the ligand revealed that it possesses excellent oral bio-availability and pharmacokinetic profiles. In addition, quantum mechanical calculations on ligand Y-1 reveals a HOMO–LUMO energy gap of 3.44 eV and global electrophilicity index ( $\omega$ ) of 1.47 eV. The high energy gap and low value of  $\omega$  are indicative of its sound kinetic and thermodynamic stabilities, which are crucial requirements of an ideal drug. The findings of this study could provide an excellent platform for developing novel antibiotics that could curb the ugly trend of multidrug resistance by *Salmonella typhi*.

### Abbreviations

ADMET	Absorption, distribution, metabolism, excretion, toxicity
BBB	Blood brain barrier
cLogP	Consensus octanol water partition coefficient
GIA	Gastrointestinal absorption
HBA	Hydrogen bond acceptor
HBD	Hydrogen bond donor

HOMO	Highest occupied molecular orbital
LUMO	Lowest unoccupied molecular orbital
Mw	Molecular weight
NRB	Number of rotatable bond
P-gp <sup>+</sup>	P-glycoprotein substrate
SBDD	Structure based drug design
SipA	Salmonella invasion protein A
TPSA	Topological polar surface area

### Acknowledgements

We appreciate the technical support of the staff and Postgraduate students of the Physical Chemistry Unit of Ahmadu Bello University Zaria, Nigeria

### Author contributions

AU prepared the research outline. APJ performed the research and drafted the manuscript. The research was supervised by AU, GAS, and SU. In addition, the manuscript was read and approved by all the authors.

### Funding

This research did not receive any specific grant from funding agencies in the public, commercial, or not-for-profit sectors.

### Availability of data and materials

The source of the data and materials used in this study has been duly acknowledged in the manuscript.

### Declarations

#### Ethics approval and consent to participate

This item is not applicable to this study.

#### Consent for publication

The authors provide consent to publish the manuscript.

#### Competing interests

The authors declare that they have no competing interests.

Received: 6 February 2023 Accepted: 7 February 2024

Published online: 12 February 2024

### References

- Talele TT, Khedkar SA, Rigby AC (2010) Successful applications of computer aided drug discovery: moving drugs from concept to the clinic. *Curr Top Med Chem* 10:127–141. <https://doi.org/10.2174/156802610790232251>
- Computational Chemists Take Nobel Prize. <https://www.chemistryworld.com/news/computational-chemists-take-nobel-prize/6676.article>. Accessed 14 Jan 2023
- World Health Organization (WHO) Fact Sheet. 2018. Available online: <https://www.who.int/news-room/fact-sheets/detail/antibiotic-resistance>. Accessed 20 Sept 2022
- De Kraker MEA, Stewardson AJ, Harbarth S (2016) Will 10 million people die a year due to antimicrobial resistance by 2050? *PLoS Med* 13:e1002184. <https://doi.org/10.1371/journal.pmed.1002184>
- Akter T, Chakma M, Tanzina AY, Rumi MH, Shimu MSS, Saleh MA et al (2022) Curcumin analogs as a potential drug against antibiotic resistant protein,  $\beta$ -Lactamases and L, D-transpeptidases involved in toxin secretion in *Salmonella typhi*: a computational approach. *Biomedinformatics* 2:77–100. <https://doi.org/10.3390/biomedinformatics2010005>
- Crump JA, Mintz ED (2010) Global trends in typhoid and paratyphoid fever. *Clin Infect Dis* 50:241–246. <https://doi.org/10.1086/649541>
- Naheed A, Ram PK, Brooks WA, Hossain MA, Parsons MB, Talukder KA et al (2010) Burden of typhoid and paratyphoid fever in a densely populated urban community, Dhaka, Bangladesh. *Int J Infect Dis* 14:e93–e99. <https://doi.org/10.1016/j.ijid.2009.11.023>

8. Stanaway JD, Reiner RC, Blacker BF, Goldberg EM, Khalil IA, Troeger CE et al (2019) The global burden of typhoid and paratyphoid fevers: a systematic analysis for the Global Burden of Disease Study 2017. *Lancet Infect Dis* 19:369–381. [https://doi.org/10.1016/S1473-3099\(18\)30685-6](https://doi.org/10.1016/S1473-3099(18)30685-6)
9. Parry CM, Hien TT, Dougan G, White NJ, Farrar JJ (2002) Typhoid fever. *N Engl J Med* 347:1770–1782. <https://doi.org/10.1056/NEJMra020201>
10. Ameji PJ, Uzairu A, Shallangwa A, Uba S (2022) Molecular docking study and insilico design of novel drug candidates against *Salmonella typhi*. *Adv J Chem-Sect B* 4:281–298. <https://doi.org/10.22034/ajcb.2022.366678.1129>
11. Skariyachan S, Jayaprakash N, Bharadwaj N, Narayanappa R (2014) Exploring insights for virulent gene inhibition of multidrug resistant *Salmonella typhi*, *Vibrio cholerae*, and *Staphylococcus aureus* by potential phytoligands via in silico screening. *J Biomol Struct Dyn* 32(9):1379–1395. <https://doi.org/10.1080/07391102.2013.819787>
12. Kariuki S, Revathi G, Kiiru J, Mengo DM, Mwituria J, Muyodi J et al (2010) Typhoid in Kenya is associated with a dominant multidrug-resistant *Salmonella enterica* serovar Typhi haplotype that is also widespread in Southeast Asia. *J Clin Microbiol* 48:2171–2176. <https://doi.org/10.1128/JCM.01983-09>
13. Peirano G, Van der Blij, Freeman KA, Poirel LJ, Nordmann L, Costello P et al (2014) Characteristics of *Escherichia coli* sequence type 131 isolates that produce extended-spectrum  $\beta$ -lactamases: Global distribution of the H 30-Rx sublineage. *Antimicrob Agents Chemother* 58:3762–3767. <https://doi.org/10.1128/AAC.02428-14>
14. Smith SM, Palumbo PE, Edelson PJ (1984) *Salmonella* strains resistant to multiple antibiotics: therapeutic implications. *Pediatric Infect Dis* 3:455–460. <https://doi.org/10.1097/00006454-198409000-00017>
15. Chen S, Cui S, McDermott PF, Zhao S, White DG, Paulsen I, Meng J (2007) Contribution of target gene mutations and efflux to decreased susceptibility of *Salmonella enterica* serovar Typhimurium to fluoroquinolones and other antimicrobials. *Antimicrob Agents Chemother* 51:535–542. <https://doi.org/10.1128/AAC.00600-06>
16. Gained R, Paglietti B, Murgia M, Dawar R, Uzzau S, Cappuccinelli P, Deb M, Aggarwal P, Rubino S (2006) Molecular characterization of ciprofloxacin-resistant *Salmonella enterica* serovar Typhi and Paratyphi A causing enteric fever in India. *J Antimicrob Chemother* 58:1139–1144. <https://doi.org/10.1128/JCM.01161-08>
17. Hirose K, Hashimoto A, Tamura K, Kawamura Y, Ezaki T, Sagara H, Watanabe H (2002) DNA sequence analysis of DNA gyrase and DNA topoisomerase IV quinolone resistance-determining regions of *Salmonella enterica* serovar Typhi and serovar Paratyphi A. *Antimicrob Agents Chemother* 46:3249–3252. <https://doi.org/10.1128/AAC.46.10.3249-3252.2002>
18. Menezes GA, Harish BN, Khan MA, Goessens W, Hays J (2016) Antimicrobial resistance trends in blood culture positive *Salmonella* Paratyphi A isolates from Pondicherry, India. *Indian J Med Microbiol* 34:222–227. <https://doi.org/10.4103/0255-0857.180352>
19. Wilke MS, Lovering AL, Strynadka NC (2005)  $\beta$ -Lactam antibiotic resistance: a current structural perspective. *Curr Opin Microbiol* 8:525–533. <https://doi.org/10.1016/j.mib.2005.08.016>
20. Kore PP, Mutha MM, Antre VR, Oswal JR, Kshirsagar SS (2012) Computer-aided drug design: an innovative tool for modeling. *Open J Med Chem* 2:139–148. <https://doi.org/10.4236/ojmc.2012.24017>
21. Padole SS, Asnani JA, Chaple DR, Katre GS (2022) A review of approaches in computer-aided drug design in drug discovery. *GSC Biol Pharm Sci* 19(02):075–083. <https://doi.org/10.30574/gscbps.2022.19.2.0161>
22. Hossain S, Sarkar B, Prottoy MNI, Araf Y, Taniya MA, Ullah MA (2019) Thrombolytic activity, drug likeness property and ADME/T analysis of isolated phytochemicals from ginger (*Zingiber officinale*) using in silico approaches. *Mod Res Inflamm* 8:29–43. <https://doi.org/10.4236/mri.2019.83003>
23. Yu H, Adedoyin A (2003) ADME–Tox in drug discovery: integration of experimental and computational technologies. *Drug Discov Today* 8:852–861. [https://doi.org/10.1016/S1359-6446\(03\)02828-9](https://doi.org/10.1016/S1359-6446(03)02828-9)
24. Bueno MS, Wozniak A, Leiva ED et al (2010) *Salmonella* pathogenicity island 1 differentially modulates bacterial entry to dendritic and non-phagocytic cells. *Immunology* 130(2):273–287. <https://doi.org/10.1111/j.1365-2567.2009.03233.x>
25. Clark AM, Jepson AM, Simmons LN, Hirst HB (1994) Preferential interaction of *Salmonella typhimurium* with mouse Peyer's patch M cells. *Res Microbiol* 145(7):543–552. [https://doi.org/10.1016/0923-2508\(94\)90031-0](https://doi.org/10.1016/0923-2508(94)90031-0)
26. McGhie JE, Hayward DR, Koronakis V (2001) Cooperation between actin-binding proteins of invasive *Salmonella*: SipA potentiates SipC nucleation and bundling of actin. *EMBO J* 20(9):2131–2139. <https://doi.org/10.1093/emboj/20.9.2131>
27. Finlay BB, Gumbiner B, Falkow S (1998) Penetration of *Salmonella* through a polarized Madin-Darby canine kidney epithelial cell monolayer. *J Cell Biol* 107(1):221–230. <https://doi.org/10.1083/jcb.107.1.221>
28. Guttman JA, Finlay BB (2009) Tight junctions as targets of infectious agents. *Biochem Biophys Acta* 1788(4):832–841. <https://doi.org/10.1016/j.bbamem.2008.10.028>
29. Garcia-del Portillo F, Núñez-Hernández C, Eisman B, Ramos-Vivas J (2008) Growth control in the *Salmonella*-containing vacuole. *Curr Opin Microbiol* 11(1):46–52. <https://doi.org/10.1016/j.mib.2008.01.001>
30. Al-Majedy YK, Kadhum AAH, Al-Amiery AA, Mohamad AB (2017) Coumarins: the antimicrobial agents. *Syst Rev Pharm* 8(1):62–70. <https://doi.org/10.5530/srp.2017.1.11>
31. Thakur S, Ray S, Jhunjhunwala S, Nandi D (2020) Insights into coumarin-mediated inhibition of biofilm formation in *Salmonella typhimurium*. *Biofouling* 36(4):479–491. <https://doi.org/10.1080/08927014.2020.1773447>
32. Ng TB, Ling JM, Wang ZT, Cai JN, Xu GJ (1996) Examination of coumarins, flavonoids and polysaccharopeptide for antibacterial activity. *Gen Pharmacol* 27(7):1237–1240. [https://doi.org/10.1016/0306-3623\(95\)02143-4](https://doi.org/10.1016/0306-3623(95)02143-4)
33. Rehman SU, Chohan ZH, Gulnaz F, Supuran CT (2005) In-vitro antibacterial, antifungal and cytotoxic activities of some coumarins and their metal complexes. *J Enzyme Inhib Med Chem* 20(4):333–340. <https://doi.org/10.1080/14756360500141911>
34. Lad BH, Giri RR, Chovatiya LY, Brahmabhatt ID (2015) Synthesis of modified pyridine and bipyridine substituted coumarins as potent antimicrobial agents. *J Serb Chem Soc* 80(6):739–747. <https://doi.org/10.2298/JSC140804004L>
35. Ameji JP, Uzairu U, Shallangwa GA, Uba S (2022) Virtual screening of novel pyridine derivatives as effective inhibitors of DNA gyrase (GyrA) of *Salmonella typhi*. *Curr Chem Lett* 12:1–16. <https://doi.org/10.5267/j.ccl.2022.10.002>
36. Lipinski CA (2004) Lead and drug-like compounds: the rule of five revolution. *Drug Discov Today Technol* 1(4):337–341. <https://doi.org/10.1016/j.ddtec.2004.11.007>
37. Verber DF, Johnson SR, Cheng HY, Smith BR, Ward KW, Kopple KD (2002) Molecular properties that influence the oral bioavailability of drug candidates. *J Med Chem* 45(12):2615–2623. <https://doi.org/10.2021/jm020017n>
38. Yu W, MacKerell AD Jr (2017) Computer-aided drug design methods. *Methods Mol Biol* 1520:85–106. [https://doi.org/10.1007/978-1-4939-6634-9\\_5](https://doi.org/10.1007/978-1-4939-6634-9_5)
39. Macalino SJY, Gosu V, Hong S, Choi S (2015) Role of computer-aided drug design in modern drug discovery. *Arch Pharm Res* 38:1686–1701. <https://doi.org/10.1007/s12272-015-0640-5>
40. Halls MD, Velkovski J, Schlegel HB (2001) Harmonic frequency scaling factors for Hartree-Fock, S-VWN, B-LYP, B3-LYP, B3-PW91 and MP2 with the Sadleir pVTZ electric property basis set. *Theor Chem Acc* 105(6):413–421. <https://doi.org/10.1007/s002140000204>
41. Senosiain JP, Klippenstein SJ, Miller JA (2005) The reaction of acetylene with hydroxyl radicals. *J Phys Chem A* 109:6045–6055. <https://doi.org/10.1021/jp050737g>
42. Miar M, Shiroudi A, Pourshamsian K, Olliaey RA, Hatamjafari F (2021) Theoretical investigations on the HOMO–LUMO gap and global reactivity descriptor studies, natural bond orbital, and nucleus-independent chemical shifts analyzes of 3-phenylbenzo[d]thiazole-2(3H)-imine and its para-substituted derivatives: solvent and substituent effects. *J Chem Res*. <https://doi.org/10.1177/1747519820932091>
43. Padmaja L, Ravikumar C, Sajjan D, Joe HI et al (2009) Density functional study on the structural conformations and intramolecular charge transfer from the vibrational spectra of the anticancer drug combretastatin-A2. *J Raman Spectrosc* 40:419–428. <https://doi.org/10.1002/jrs.2145>
44. Ruiz-Morales Y (2002) HOMO–LUMO gap as an index of molecular size and structure for polycyclic aromatic hydrocarbons (PAHs) and

- asphaltenes: a theoretical study. *J Phys Chem A* 106:11283–11308. <https://doi.org/10.1021/jp021152e>
45. Boyle CE, Brown FN, Finlay BB (2006) Salmonella enterica serovar Typhimurium effectors SopB, SopE, SopE2 and SipA disrupt tight junction structure and function. *Cell Microbiol* 8(12):1946–1957. <https://doi.org/10.1111/j.1462-5822.2006.00762.x>
  46. Tian S, Wang J, Li Y, Li D, Xu L, Hou T (2015) The application of in silico drug-likeness predictions in pharmaceutical research. *Adv Drug Deliv Rev* 86:1–10. <https://doi.org/10.1016/j.addr.2015.01.009>
  47. Wang Y, Xing J, Xu Y, Zhou N, Peng J, Xiong Z, Liu X, Luo X, Luo C, Chen K (2015) In silico ADME/T modeling for rational drug design. *Q Rev Biophys* 48:488–515. <https://doi.org/10.1017/S0033583515000190>
  48. Daina A, Michielin O, Zoete V (2017) SwissADME: a free web tool to evaluate pharmacokinetics, druglikeness and medicinal chemistry friendliness of small molecules. *Sci Rep* 7:42717. <https://doi.org/10.1038/srep42717>
  49. Anzenbacher P, Anzenbacherova E (2001) Cytochromes P450 and metabolism of xenobiotics. *Cell Mol Life Sci CMLS* 58:737–747. <https://doi.org/10.1007/pl00000897>
  50. De Graaf C, Vermeulen NP, Feenstra KA (2005) Cytochrome P450 in silico: an integrative modeling approach. *J Med Chem* 48:2725–2755. <https://doi.org/10.1021/jm040180d>
  51. Lamb DC, Waterman MR, Kelly SL, Guengerich FP (2007) Cytochromes P450 and drug discovery. *Curr Opin Biotechnol* 18:504–551. <https://doi.org/10.1016/j.copbio.2007.09.010>
  52. Kurt M, Sertbakan TR, Ozduran M (2008) Spectrochim: an experimental and theoretical study of molecular structure and vibrational spectra of 3- and 4-pyridineboronic acid molecules by density functional theory calculations. *Spectrochim Acta Part A Mol Biomol Spectrosc* 70:664–673. <https://doi.org/10.1016/j.saa.2007.08.019>
  53. Pearson RG (1992) Chemical hardness and electronic chemical potential. *Inorg Chim Acta* 198(200):781–786. [https://doi.org/10.1016/S0020-1693\(00\)92423-x](https://doi.org/10.1016/S0020-1693(00)92423-x)

### Publisher's Note

Springer Nature remains neutral with regard to jurisdictional claims in published maps and institutional affiliations.